

Investigation of Acrylamide Based Hydrogels as L-Dopa and L-Tyrosine Drug Release System

İdil Karaca Açıarı*

Bioengineering Department, Faculty of Engineering and Natural Sciences, Malatya Turgut Özal University,
44210, Malatya, Turkey.
idil.karaca@ozal.edu.tr*

(Received on 23rd Feb 2022, accepted in revised form 26th May 2022)

Summary: Acrylamide-based hydrogels exhibit significant volume migration in response to physical and chemical stimuli. These properties make their use as drug delivery systems widespread. In the study, acrylamide-based hydrogel structures were synthesized to be used as two prodrugs known as L-Dopa and L-Tyrosine carrier and release system. Fourier-transform infrared (FTIR) spectroscopy, scanning electron micrography (SEM), Image J program were used to evaluate the structure-property relationship of the synthesized hydrogels and swelling studies were performed. The maximum swelling capacity of the synthesized hydrogel structures was determined as 973.80 ± 12.25 %. The L-Dopa loading on the hydrogel was 69.51 ± 9.64 % and the L-Tyrosine loading was 61.37 ± 5.08 %. The release behavior of the drugs loaded on the hydrogel was monitored using a UV-vis spectrophotometer at pH 7.4 and λ_{\max} 280 nm. Accordingly, it was observed experimentally that 84.21 ± 1.71 % of L-Dopa and 75.98 ± 2.69 % of L-Tyrosine were released. The study is an alternative release system with the simultaneous release of L-Dopa molecule, which is especially used in the treatment of Parkinson's disease, and L-Tyrosine, which plays an important role in the synthesis of L-Dopa.

Keywords: Acrylamide-based hydrogels, L-Dopa, L-Tyrosine, Drug release system.

Introduction

Hydrogels are defined as a three-dimensional cross-linked polymeric network obtained from water-insoluble synthetic or natural polymers that have the ability to absorb large amounts of water or biological fluid in the body due to the presence of hydrophilic groups in their structure [1-6]. Examples of natural hydrogels are protein collagen and gelatin, polysaccharide agarose and alginate. Acrylic acid (AAc), acrylamide (AAm), hydroxyethyl methacrylate (HEMA), methacrylic acid (MAA), methyl methacrylate (MMA) can be given as examples of synthetic hydrogels [7]. Acrylic acid and acrylamide are the main materials used in the synthesis of hydrogels [8]. The water holding capacity of hydrogels is mainly due to the presence of hydrophilic groups [9]. Hydrophilic functional groups in the main polymer chain of hydrogels include hydroxyl groups (OH⁻), carboxyl (COOH⁻), amine (NH₂) and sulfate (SO₃H⁻) [10]. Hydrogels have now received increasing attention from many of the scientists in different research fields. Hydrogels have played an important role in a wide variety of applications, including drug delivery systems, diagnostics, tissue engineering, optics and imaging [9]. Hydrogels have remarkable porosity and compatibility with aqueous media. This feature provides important advantages to hydrogels, especially as drug delivery systems [11]. In addition to this advantage, it is known that the widely used polyacrylamide-based hydrogels do not have any toxic effects on human fibroblasts and their

biocompatibility [12]. Acrylamide-based hydrogels have an important function in solid and liquid preparations, extended and controlled release systems, capsule production, gel and bioadhesive preparations [13-14]. Recently, different applications of acrylamide hydrogel structures in controlled release systems have emerged. For example, Prusty *et al.* synthesized a nano silver-embedded soy protein polyacrylamide (PAM-SP@Ag) nanocomposite hydrogel for the release of ciprofloxacin drugs. It was determined that the in vitro drug release rate of ciprofloxacin was 95.3% in a time period of 6 hours for these synthesized hydrogel structures [15]. Mahde *et al.* studied the adsorption of aspirin drug on polyacrylamide (PAAm) hydrogel structures at different temperatures (15, 25 ve 37°C) and different pH (1.2, 4.0, 7.2) ranges. It was found that the degree of adsorption of aspirin on the hydrogel increased with decreasing temperature. It was determined that the amount of drug adsorbed on the hydrogel surface was higher at low pH [16]. Sharifzadeh *et al.* synthesized a montmorillonite-based polyacrylamide hydrogel for vaginal drug delivery. Sustained release system for 15 days with synthesized hydrogel [17]. In this study, acrylamide-based hydrogel structures were synthesized for the release of L-Dopa (3,4-dihydroxy-L-phenylalanine) and L-Tyrosine (3-(4-hydroxyphenyl)-L-alanine). It was observed that 84.21 ± 1.71 % of L-Dopa and 75.98 ± 2.69 % of L-Tyrosine were released during the release followed for 2 days in the synthesized hydrogel

*To whom all correspondence should be addressed.

structure. When we look at acrylamide-based hydrogel release systems, this study has advantages such as ease of synthesis, less cost potential than other designs, and the loaded drugs have not been used in acrylamide-based hydrogel release systems before. L-Dopa and L-Tyrosine used in the study are frequently included in the approaches to the treatment of Parkinson's disease [18-20]. L-Dopa has been recognized as an effective standard drug for the treatment of Parkinson's disease, a common neurodegenerative disorder. Parkinson's disease is a degenerative disorder associated with decreased dopamine levels in the brain that causes stiffness, tremors, slow speech, and eventually dementia [19]. In Parkinson's disease, dopamine levels drop. With this reduction, direct administration of dopamine is not beneficial as dopamine does not cross the blood-brain barrier, but L-Dopa, a precursor of dopamine, can cross the blood-brain barrier and be converted to dopamine, thus relieving Parkinson's patients [18, 19]. L-Dopa can initiate protein misfolding through its ability to mimic the protein amino acid L-Tyrosine, resulting in random errors in aminoacylation and inadvertent addition of L-Dopa to the polypeptide chain of proteins instead of L-Tyrosine. The use of L-Dopa in combination with L-Tyrosine can provide full protection against these effects. It has been suggested that co-treatment with L-Tyrosine may be therapeutically beneficial, supporting the view that incorrect binding of L-Dopa to proteins contributes to these cytotoxic effects [20].

In this study, acrylamide-based hydrogel structures were prepared in which L-Dopa and L-Tyrosine drugs were loaded and released. The parameters of the prepared hydrogel structures such as characterization, surface morphology, swelling, drug loading-release were determined.

Experimental

Materials

L-Dopa (SIGMA), L-Tyrosine (Sigma-Aldrich, reagent grade $\geq 98\%$) and other chemical and organic solvents used in the study were obtained from Merc. Sigma aldrich brand 43mm x 27mm dialysis membrane was used in the drug release phase.

Instrumentation

In the study, Perkin Elmer 283 model FTIR spectrophotometer was used for structural characterization. FTIR analysis was performed with a spectral sensitivity of 4 cm^{-1} and a wavelength range of $400\text{-}4000\text{ cm}^{-1}$. The surface properties and morphologies of the hydrogels were examined with

SEM (LEO Evo-40 VPX) device. ImageJ program was used to analyze the microstructure of hydrogels [21]. In the experimental processes, the solvent removal in the hydrogel structures was removed by using the Freeze Dryer brand BK-FD12S (-80°C) model lyophilizer and the drying process was carried out. Drug loading and release studies were performed with a UV spectrophotometer (UV-1601 Shimadzu).

Pore Size and Pore Area Calculation with ImageJ Program

The pore distributions of the synthesized hydrogels were analyzed in ImageJ version 1.53k. In these examinations, a histogram graph was obtained by examining the SEM photograph at 1.00KX magnification and measuring all pore diameters in the hydrogel structure on the Image. Histogram maximum values were considered as the optimum pore diameter. Experimentally, firstly, the synthesized hydrogel structures were dried with a lyophilizer. SEM images were obtained at different magnifications by taking thin sections from different regions on the lyophilized hydrogel structures. These SEM images were sized with the ImageJ program and histogram graphics were obtained by performing an average of 180 dimension analysis from each image. Mathematical area measurements were made by using pore diameters in the pore area calculation. Area measurements were calculated using the program.

Synthesis of Hydrogels

Acrylamide was used as monomer and 10 % bisacrylamide was used as crosslinking agent for the synthesis of acrylamide-based hydrogels. In order to initiate the related synthesis, benzoyl peroxide was preferred as the radical initiator. Solution polymerization technique was used in hydrogel synthesis. THF was chosen as the solvent.

Acrylamide (AAM) 90.7 % (wt.), bisacrylamide (BAAM) 9.07 % (wt.) and benzoyl peroxide (BPO) dissolved in 0.18 % (wt.) THF. Polymerization was initiated by adding BPO solution. After passing through a nitrogen atmosphere for 15 minutes, the reaction was run in a reflux system. The mixture was held at 70°C for 3 hours. Several washes with deionized water were performed to remove the uncrosslinked polymer and unreacted monomers from the hydrogels. The cleared gels were dried in a lyophilizer. Structural characterization, surface morphologies and surface micromorphological features of hydrogels were determined with appropriate techniques.

Swelling Capacity

For swelling measurements, approximately 0.05 g of hydrogel was placed in deionized (DI) water. Weight gain was monitored at room temperature by weighing the material periodically removed from the DI water. The swollen gels were weighed with an electronic balance. Inflation studies were carried out until equilibrium in swelling was reached. Each measurement was repeated at least three times. The swelling rate was calculated using the following equation.

$$\text{Swelling ratio (\%)} = [(W_s - W_d)/W_d] \times 100$$

where, W_s (swollen) is the measured weight of material after contact with DI water, and W_d (dry) is the measured weight of dry material [22].

Drug Release Studies

Determining Maximum Absorption Wavelength for L-Dopa and L-Tyrosine

Before monitoring L-Dopa and L-Tyrosine release with UV spectrophotometer, the maximum absorption wavelength of L-Dopa and L-Tyrosine were determined. For this, samples prepared in different concentrations were subjected to scanning in the 250-400 nm range.

L-Dopa and L-Tyrosine Loading and Release Studies

Pre-weighed hydrogels (200 mg) were placed in a prepared solution of 20 mL of aqueous L-Dopa (1 mg/mL) and 20 mL of aqueous L-Tyrosine (1 mg/mL) prepared for 2 hours, and hydrogel structures were incubated in the shaker system for 24 hours [23]. The amount of L-Dopa and L-Tyrosine loaded was determined using a UV-vis spectrophotometer at λ_{max} 280 nm. Drug release studies were performed at 37 °C in 20 mL of PBS buffer (pH 7.4). In order to determine the amount of drug released at certain time intervals, the hydrogel samples left in the dialysis bag were monitored using a UV-vis spectrophotometer at λ_{max} 280 nm for 48 hours with continuous mixing at 50 rpm in an environment containing phosphate buffer at 37 °C pH 7.4 [24]. All experimental steps were performed in triplicate.

Results and Discussion

Characterization of Hydrogel and L-Dopa and L-Tyrosine Loaded Hydrogel Structures

FTIR spectra are given in Figs. 1 and 2. L-Dopa spectra show peaks at 3060.79 cm^{-1} , 1651.83 cm^{-1} and 1456.12 cm^{-1} , which are properties of the pure drug. The peak at 1651.83 cm^{-1} represents the di-substituted aromatic ring, while the peak at 1456.12 cm^{-1} represents the O-H stretching from the carboxylic acid group on the drug. Also, the peak at 3060.79 cm^{-1} indicates the amine group in the drug molecule. Spectra are consistent with

the literature [25-27]. FTIR spectra of the polyacrylamide-based hydrogel show the presence of absorption bands characteristic to crosslinking bridges. In the spectrums of the hydrogel structure are observed as absorption bands assigned to deformation vibration of -CH₂ groups at 1051.23 cm^{-1} , absorption bands assigned to deformation vibration of -C-N- links at 1426.07 cm^{-1} , N-H stretching vibration originating from the amidic group at 1543.44 cm^{-1} , C=O stretching vibration originating from the amidic group at 1657.96 cm^{-1} , absorption band of the -NH group at 3311.89 cm^{-1} [28]. When we look at the L-Dopa-loaded hydrogel structures, the band with a center of 3185.06 cm^{-1} is due to the presence of -NH₂ and -OH groups in the amino acid. A very broad peak at 1648.17 cm^{-1} represents the characteristic aromatic ring for L-Dopa. This is evidence of L-Dopa loading in the hydrogel. In addition, an absorption band associated with carboxylate is observed at 1420.24 cm^{-1} in the spectra of the L-Dopa loaded hydrogel. When the FTIR spectrum for L-Tyrosine was examined, O-H stretching was observed at 3200.68 cm^{-1} corresponding to the carboxyl acid hydroxyl group and the alcoholic hydroxyl group of the L-Tyrosine molecule. A low, narrow peak at 2929.75 cm^{-1} indicates C-H stretching. The bands at 1606.09 cm^{-1} , 1328.85 cm^{-1} and 1154.07 cm^{-1} represent N-H stretching, aromatic C-H stretching vibration and C-O phenolic groups, respectively. The groups of peaks associated with it are due to -COO- vibrations. The para substitution in the aromatic ring is confirmed by the peak at 839.74 cm^{-1} in spectrum. Spectra are consistent with the literature [29, 30]. A wide peak is observed at 3200.29 cm^{-1} in the spectra of the L-Tyrosine loaded hydrogel. This wide peak is interpreted as the O-H stretch corresponding to the L-Tyrosine-derived carboxylic acid hydroxyl group and the alcoholic hydroxyl group. Spectrums were observed as C=O stretching vibration originating from the amidic group of the peak at 1655.02 cm^{-1} , stretching vibration of the -COO- group at 1451.60 cm^{-1} , aromatic C-H stretching vibration at 1325.56 cm^{-1} and absorption bands assigned to the deformation vibrations of -CH₂ groups at 1078.12 cm^{-1} . It is seen that these peaks are added to the spectrum due to the L-Tyrosine group. The hydrogel was loaded with L-Tyrosine.

SEM Images and Microstructure Studies

Microstructures of freeze-dried hydrogels were visualized by SEM. We see SEM images of acrylamide-based hydrogel structures at different magnifications in Fig. 3. The porous and interconnected sponge-like structures of hydrogels with micrometric pore diameters are clearly visible [31].

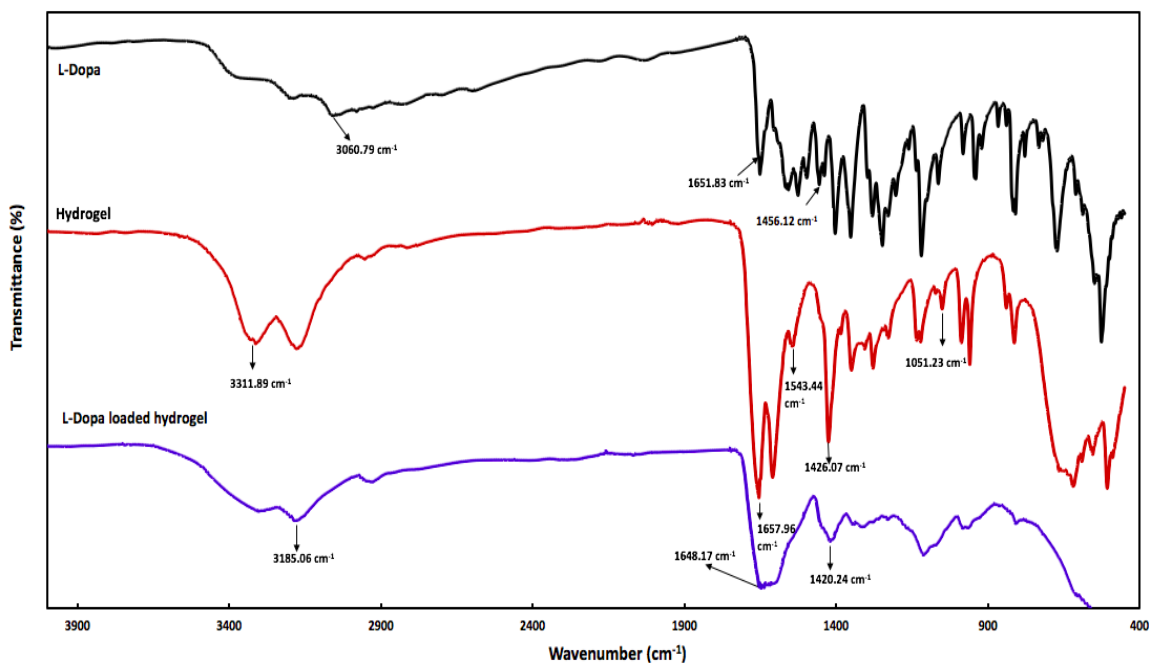


Fig. 1: FTIR spectrum of L-Dopa, Hydrogel and L-Dopa loaded hydrogel.

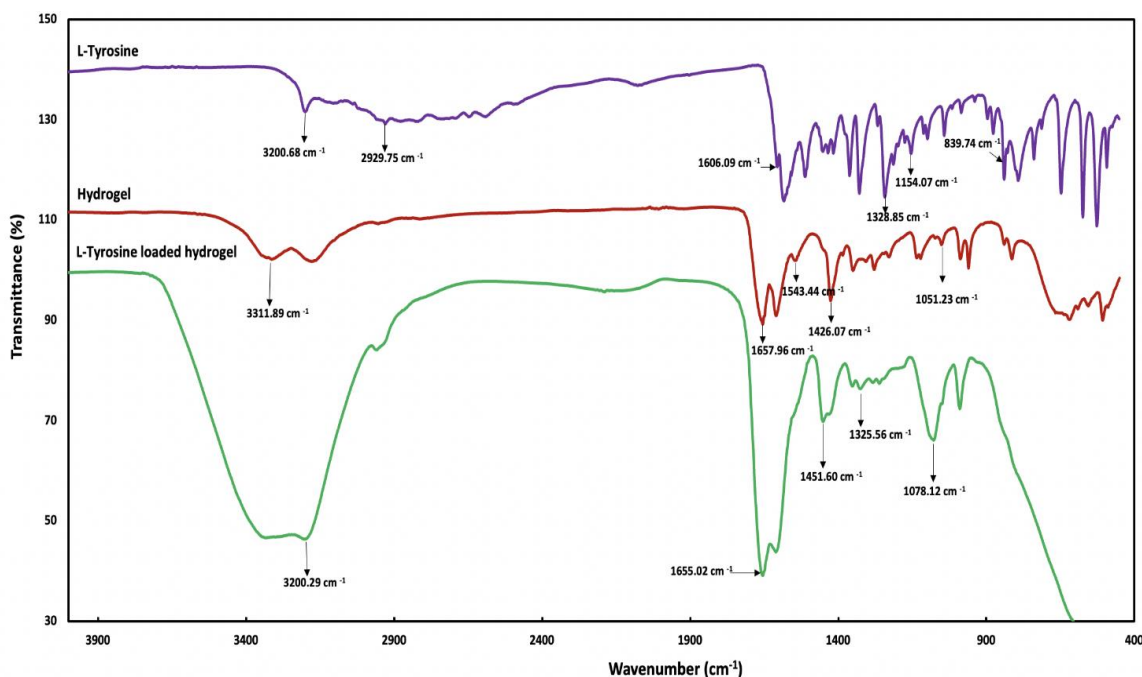


Fig. 2: FTIR spectrum of L-Tyrosine, Hydrogel and L-Tyrosine loaded hydrogel.

In addition, the pore areas and pore lengths of the hydrogels are given in Fig.4. The average area of the pores was $83.24 \mu\text{m}^2$ and the average length of the pores was $12.20 \mu\text{m}$. SEM images of the hydrogels loaded with L-Dopa and L-Tyrosine are available in Fig.5. The surface morphology of the hydrogels

changed significantly after loading with L-Dopa and L-Tyrosine. It is observed that the hydrogel structures which are highly porous and have a spongy structure before loading are filled with drugs after drug loading. The change in surface morphology is quite clear.

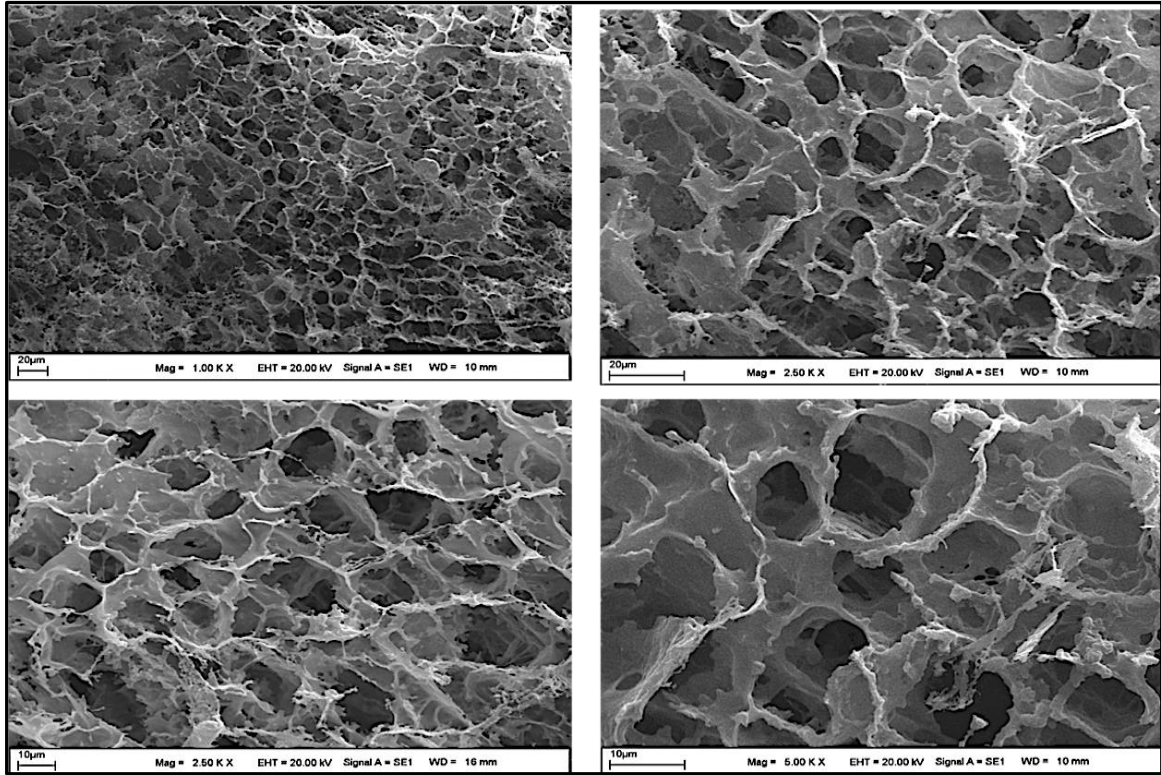


Fig. 3: SEM images of hydrogel structure with different magnification.

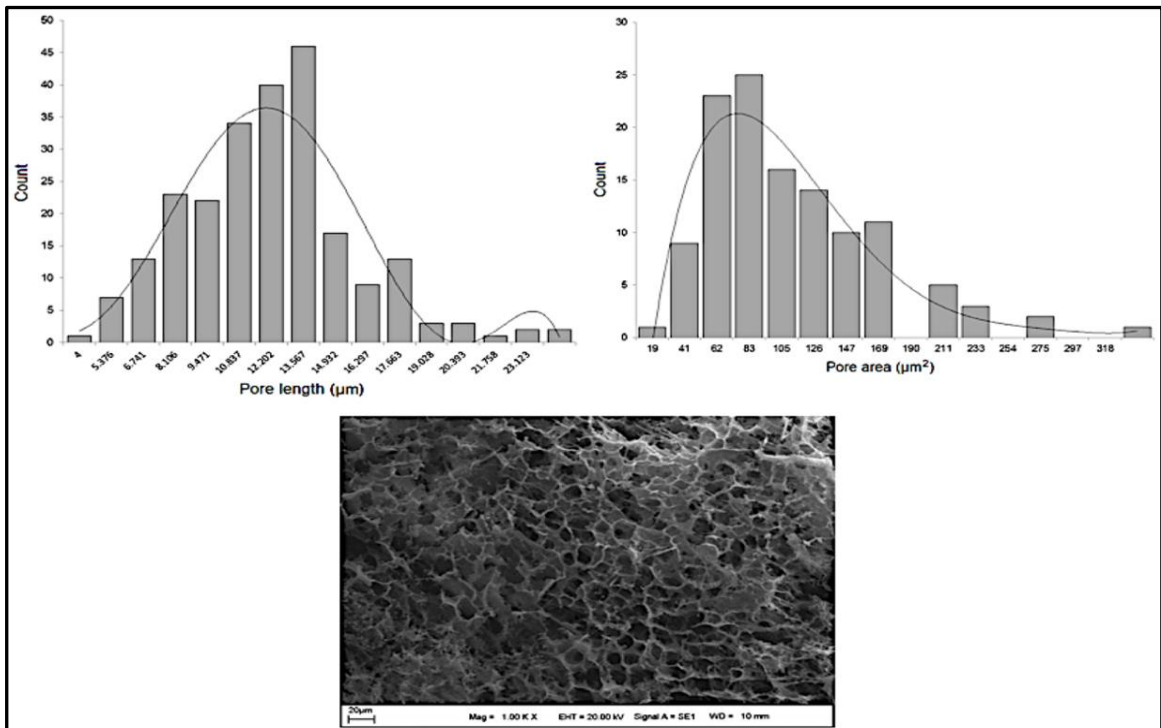


Fig. 4: Micromorphological Properties of hydrogel structure.

Swelling Capacity Results

The swelling rate is one of the most important parameters to evaluate the effectiveness of hydrogel materials. When the dry hydrogel is placed in water, the water will penetrate into the gel and hydrate the polar hydrophilic groups in the structure. But when it reaches a certain point, it encounters the resistance of the cross-linkers in the network structure. The gel stops swelling at this point. The water absorption of

hydrogels at different time intervals is given in Fig. 6. Percent swelling rates of the hydrogel were monitored in DI water for 24 hours. It has been noted that hydrogels initially absorb a large amount of water and then increase slightly over time. Percent swelling rate was $136.82 \pm 14.87\%$ at 30th minute, $644.53 \pm 14.60\%$ at 120th minute, $941.36 \pm 19.46\%$ at 240th minute. The maximum swelling capacity was reached at the 360th minute (Fig.6.) and the percent swelling rate was $973.80 \pm 12.25\%$.

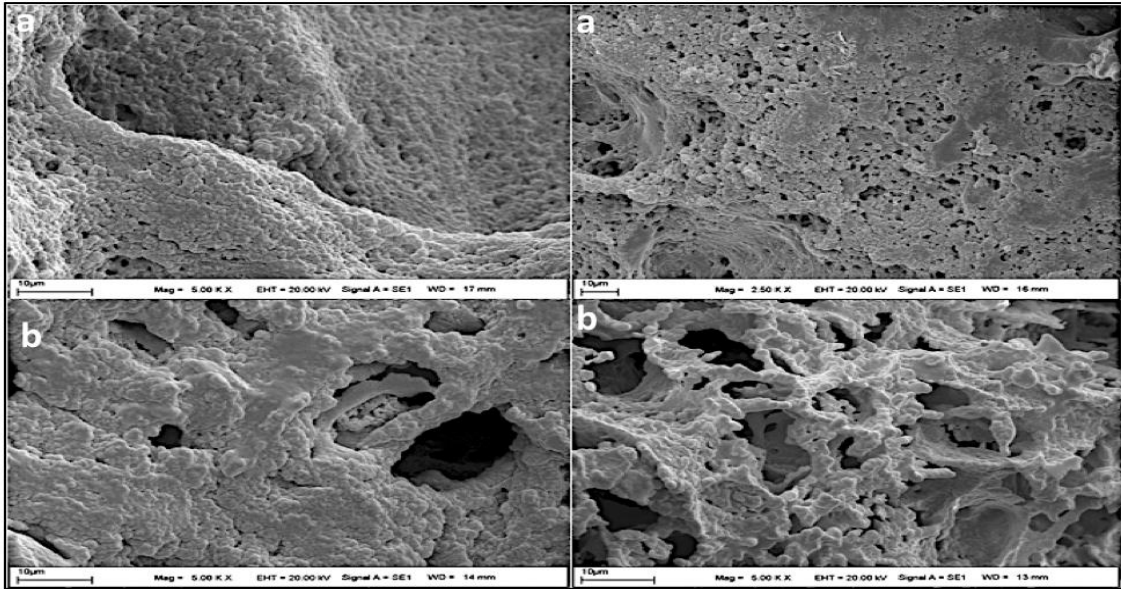


Fig. 5: SEM images of L-Dopa (a) and L-Tyrosine (b) loaded hydrogel structures with different magnification.

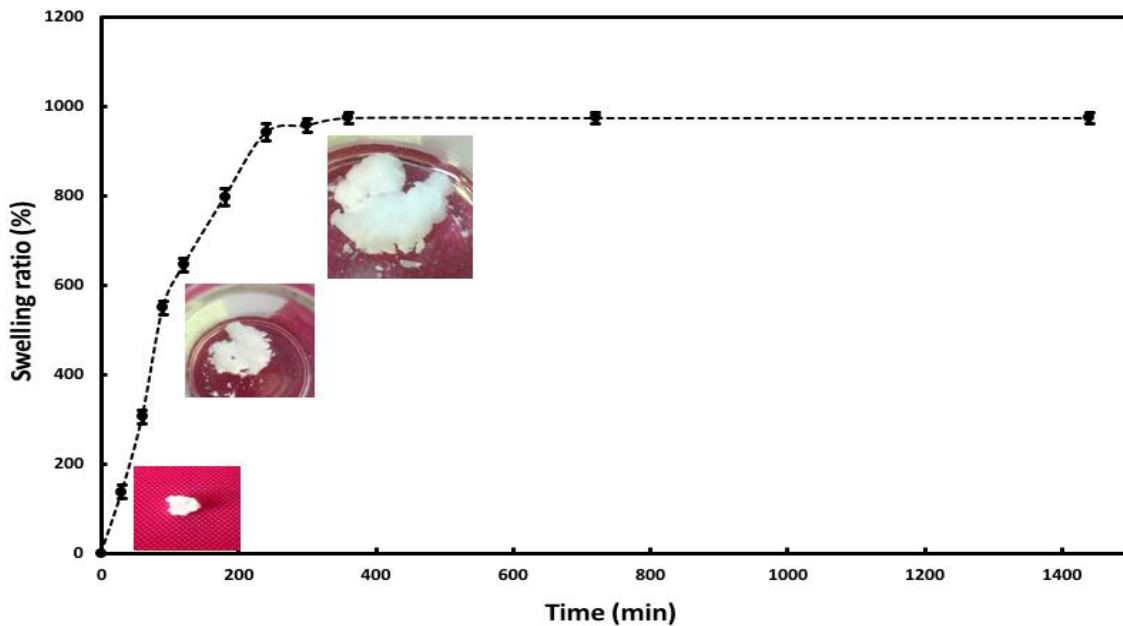


Fig. 6: Swelling ratio (%) of hydrogel.

Determining Maximum Absorption Wavelength for L-Dopa and L-Tyrosine

L-Dopa and L-Tyrosine samples at different concentrations prepared in PBS buffer were scanned in the wavelength range of 250-400 nm. Fig.7. shows the wavelength range scan for L-Dopa and L-Tyrosine. The best UV absorption spectrum was determined as the 280 nm wavelength given in Fig.7. After this determination, the drug release studies were carried out at 280 nm.

Calibration Graphs for L-Dopa and L-Tyrosine

Calibration graphs were drawn for L-Dopa and L-Tyrosine covering different concentration ranges (3-250 $\mu\text{g/mL}$) before proceeding with the drug release study. Solutions of L-Dopa and L-Tyrosine

were prepared in PBS (pH 7.4). Calibration graphs of L-Dopa and L-Tyrosine structures are given in Fig. 8(a) and Fig. 8(b) respectively.

L-Dopa and L-Tyrosine Loading and Release Studies on Hydrogel

The amounts of L-Dopa and L-Tyrosine loaded on the synthesized hydrogel were $69.51 \pm 9.64\%$ and $61.37 \pm 5.08\%$, respectively. It appears that the hydrogel is loaded with L-Dopa slightly more. It can be said that the more hydrophilic nature of L-Dopa is a factor here. The % drug release data studied in PBS (pH 7.4) at 37°C at certain time intervals are given in Fig.9.

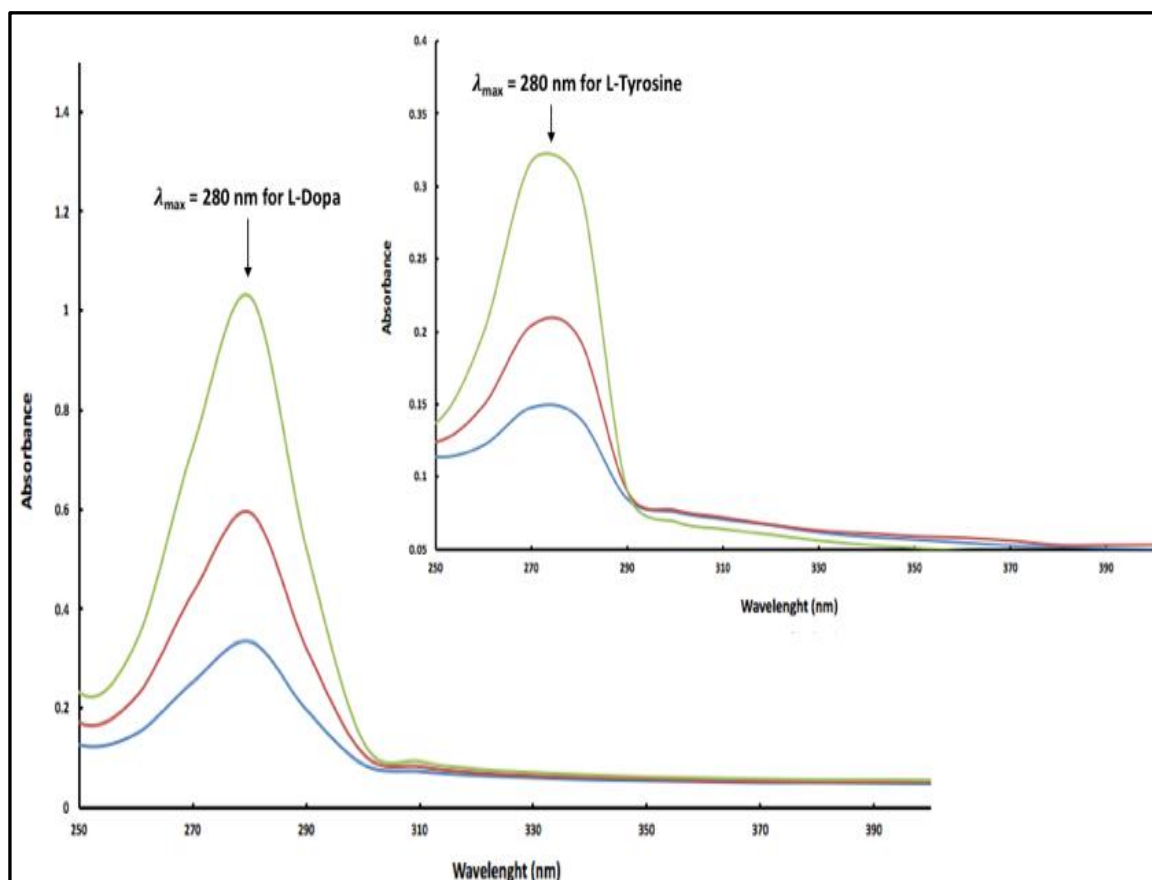


Fig. 7: Wavelength range screening for L-Dopa and L-Tyrosine.

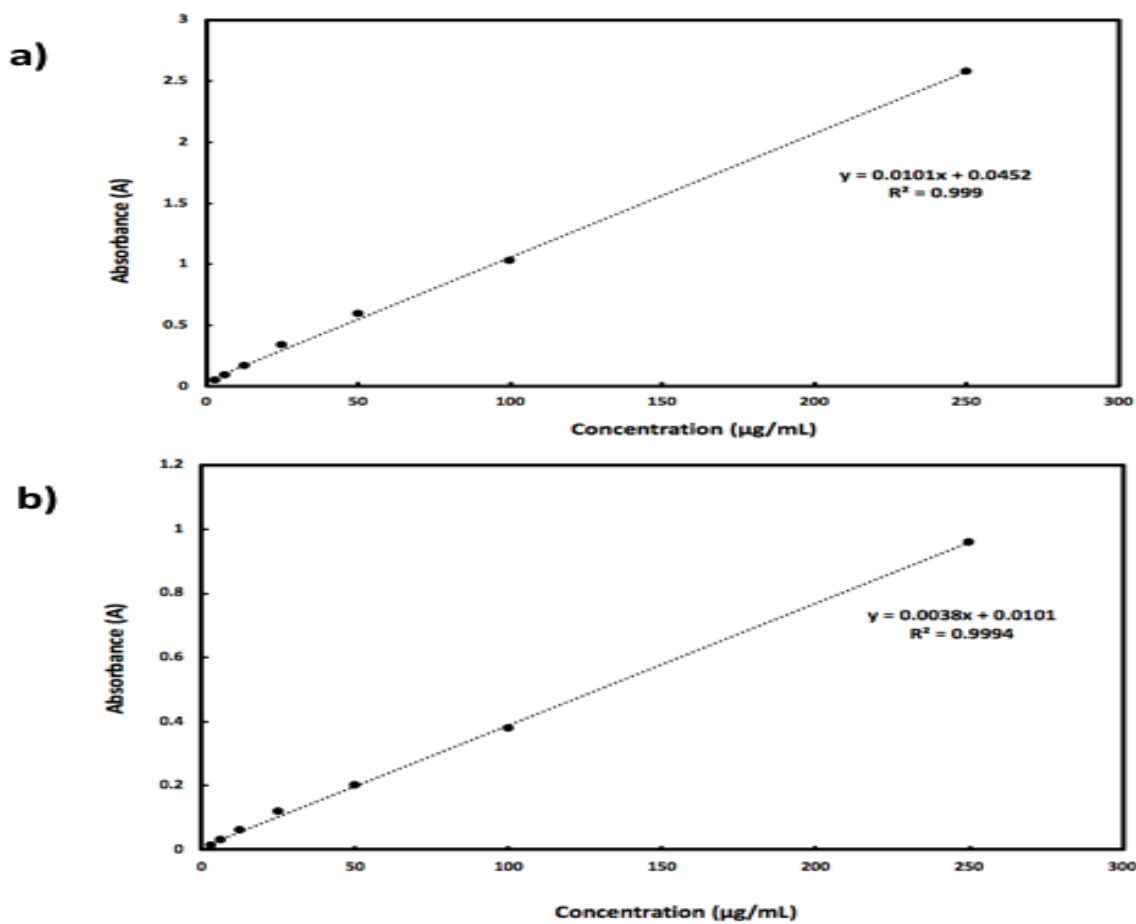


Fig. 8: Wavelength range screening for L-Dopa (a), L-Tyrosine (b).

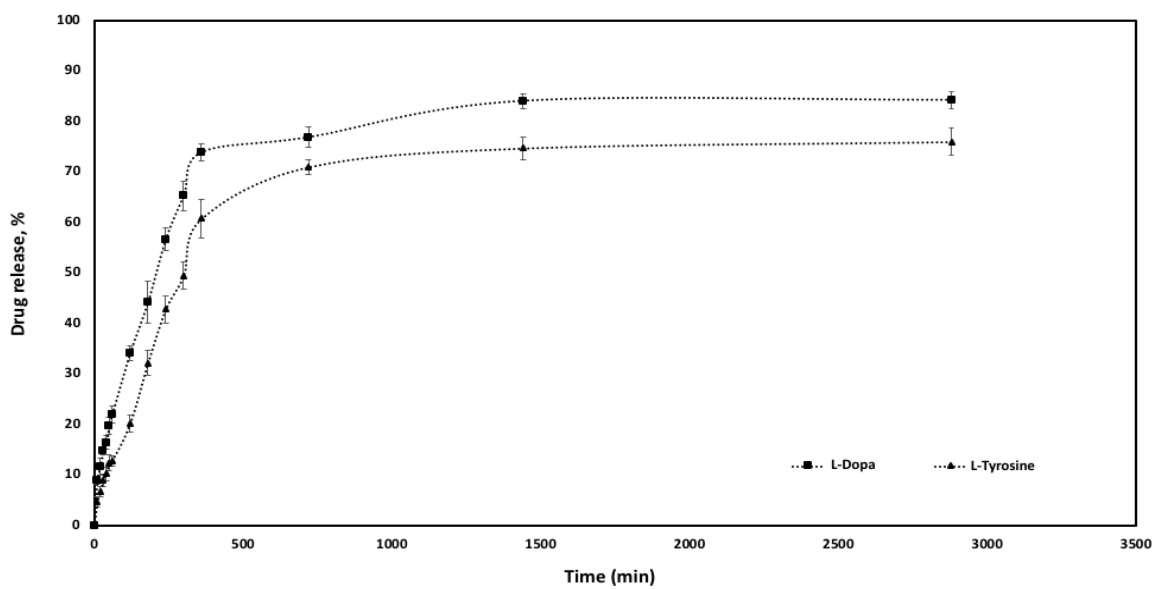


Fig. 9: Drug release (%) from hydrogels loaded with L-Dopa and L-Tyrosine.

14.82±0.82% of L-Dopa release and 8.90±1.21% of L-Tyrosine release in the first 30th minute, 21.95±1.69% of L-Dopa release and, 12.84±1.05% of L-Tyrosine release in 60th minute, 44.19± 4.21% of L-Dopa release and L-Tyrosine release 32.13±8.45% in 180th minute, L-Dopa release 73.85±1.76% and L-Tyrosine release 60.75±3.88% in 360th minute, L-Dopa release 76.83± 0.28% and L-Tyrosine release 70.98±1.52% in 720th minute, L-Dopa release 84.02±1.53% and L-Tyrosine release 74.70±2.24% in 1440th minute, L-Dopa 84.21±1.71% and L-Tyrosine release 75.98±2.69% in 2880th minute. The effect in which the drug is released at high concentrations in controlled drug release systems is called the burst effect [32]. In this study, we see the maximum drug release at the 1440th minute. When we look at the drug release percentages, we see that L-Dopa is released in higher amounts than L-Tyrosine release at the same time. We see that the hydrophilicity of L-Dopa also affects the rate of release. We see that the acrylamide-based hydrogel structure has a very good (for about 48 hours) release system for release of L-Dopa and L-Tyrosine in Fig.9. When we look at the release percentages, we see that L-Dopa is released faster. We can interpret this as being more hydrophilic than L-Tyrosine. There are acrylamide-based release systems in the literature. Acyclovir-loaded polyacrylamide-based hydrogels were synthesized by Sabbagha *et al.* [33]. Ferreira *et al.* prepared polyacrylamide hydrogels with different crosslinking densities for acetylsalicylic acid release [34]. Singh *et al.* synthesized a levofloxacin-releasing moringa gum-cl-sterculia gum-polyacrylamide hydrogel [35]. When we look at the literature, we come across many different studies for L-Dopa and L-Tyrosine releases. Sintov *et al.* developed new SANS (self-assembled nano-micelle system) formulations for transdermal administration of levodopa/carbidopa [36]. Lakouraj *et al.* synthesized a new amphiphilic hydrogel based on sodium alginate-poly pyrrole for L-Dopa release. In the synthesized hydrogel, the release of L-Dopa in acidic and basic media was determined as 60% and 80% respectively within 160 hours [37]. Bardajee *et al.* synthesized a sustained-release biopolymer-based magnetic hydrogel for levodopa (L-Dopa). The study was carried out at pH 5.4 and pH 7.4. pH systems determine model environments. pH 5.4 mimics the pH of bile, bladder and urine. pH 7.4 mimics the physiological conditions of normal tissues. They found the L-Dopa release rate to be 84% at pH 7.4 and 50% at pH 5.4 [38]. In the study, pH 7.4 was used to mimic the physiological conditions of normal tissues. Thakur *et al.* synthesized AGG-g-poly(methacrylic acid), AGG-g-poly acrylic acid, AGG-g-poly (2-hydroxyethylmethacrylate) acryloyl guar gum (AGG) based hydrogels for L-Dopa and L-Tyrosine

release. The maximum release of L-Dopa at 37 °C was observed as 25.47 % in the AGG-g-poly acrylic acid structure at the 8th hour. It was determined as 11.7 % in the structure of AGG-g-poly(methacrylic acid) in L-Tyrosine [39]. In the study, acrylamide-based hydrogel design was carried out for the release of L-Dopa and L-Tyrosine. When the literature is reviewed, the study is original and has the potential to contribute to the literature.

Conclusion

The highly porous nature of hydrogels arouses interest in their use in drug delivery applications. Its porous structure allows drugs to be loaded into the gel matrix and subsequently released.

1. Within the scope of the study, firstly acrylamide-based hydrogel structures were synthesized. L-Dopa and L-Tyrosine loadings were performed on the synthesized hydrogel structures. We observed that since L-Dopa is more hydrophilic, it is more loaded on the porous structures of hydrogels.
2. We see that the percentage of release followed for 48 hours is rapidly released from the first 30th minute, depending on the swelling rate of the gel. In the oscillation measurements after the 4th hour, we see that the oscillation is quite fast. We can say that these are the moments when the gel swells to the maximum. The gel swelled a lot and started to release the drug loaded in its structure faster.
3. The study offers an alternative to the existing release systems with the simultaneous release of L-Dopa and L-Tyrosine, which plays an important role in the synthesis of L-Dopa, which is especially used in the treatment of dopamine-deficient Parkinson's and Dopa-sensitive dystonia.
4. The resulting drug delivery system has the potential to be used in different drugs.

References

1. J. Radhakrishnan, U. M. Krishnan and S. Sethuraman, Hydrogel based injectable scaffolds for cardiac tissue regeneration, *Biotech Adv.*, **32**, 449 (2014).
2. T. Thavasyappan and D. S. Lee, Injectable hydrogels for sustained release of therapeutic agents, *J Controlled Release.*, **267**, 57 (2017).
3. A. S. Hoffman, Hydrogels for biomedical applications. *Adv Drug Del Rev.*, **64**, 18 (2012).
4. F. A. Muhammad, M. Hanif and N. M. Ranjha, Methods of synthesis of hydrogels a review, *Saudi Pharm J.*, **24**, 554 (2016).

5. I. A. Nasitha, K. Krishnakumar and B. Dineshkumar, Hydrogel in pharmaceuticals: a review, *IAJPS.*, **3**, 265 (2016).
6. N. Das, Preparation methods and properties of hydrogel: a review, *Int. J. Pharm. Pharm. Sci.*, **5**, 112 (2013).
7. A. Ulusoy and N. Dikmen, Applications of hydrogel in medicine, *Archives Medical Review Journal.*, **29**, 129 (2020).
8. G. Sennakesavan, M. Mostakhdemin, L. K. Dkhar, A. Seyfoddin and S. J. Fatihhi, Acrylic acid/acrylamide based hydrogels and its properties - A review, *Polym. Degrad. Stab.*, **180**, 109308 (2020).
9. G. R. Bharska, A review on hydrogel, *World J Pharm Pharm Sci.*, **9**, 1288 (2020).
10. A. P. Mathew, S. Uthaman, K. H. Cho, C. S. Cho and I. K. Park, Injectable hydrogels for delivering biotherapeutic molecules, *Inter J Bio Macromolecules.*, **110**, 17 (2018).
11. C. Shi, L. Zhang, H. Yin and H. Gu, Dox-loaded gelatin composite hydrogels with oxidation-triggered drug release property, *J. Chem.Soc. Pak.*, **43**, 180 (2021).
12. G. Sennakesavan, M. Mostakhdemin, L. K. Dkhar, A. Seyfoddin and S. J. Fatihhi, Acrylic acid/acrylamide based hydrogels and its properties - a review, *Polym. Degrad. Stab.*, **180**, 109308 (2020).
13. F. Sabbagha and I. I. Muhamad, Acrylamide-based hydrogel drug delivery systems: Release of Acyclovir from MgO nanocomposite hydrogel, *J Taiwan Inst Chem Eng.*, **72**, 182 (2017).
14. W. Huichao, D. Shouying, L. Yang, L. Ying and W. Di, The application of biomedical polymer material hydroxy propyl methyl cellulose (HPMC) in pharmaceutical preparations, *J Chem Pharm Res.*, **6**, 155 (2014).
15. K. Prusty, A. Biswal, S. B. Biswal and S. K. Swain, Synthesis of soy protein/polyacrylamide nanocomposite hydrogels for delivery of ciprofloxacin drug, *Mater. Chem. Phys.*, **243**, 378 (2019).
16. B. W. Mahde, N. D. Radia, L. S. Jasim and H. O. Jamel, Synthesis and characterization of polyacrylamide hydrogel for the controlled release of aspirin, *J. Pharm. Sci. & Res.*, **10**, 2850 (2018).
17. G. Sharifzadeh, H. Hezaveh, I. I. Muhamad, S. Hashim and N. Khairuddin, Montmorillonite-based polyacrylamide hydrogel rings for controlled vaginal drug delivery, *Mater. Sci. Eng. C.*, **110**, 110609 (2020).
18. S. N. Surwase and J. P. Jadhav, Bioconversion of L-tyrosine to L-DOPA by a novel bacterium *Bacillus* sp. JPI, *Amino Acids*, **41**, 495 (2011).
19. P. Agarwal, N. Pareek, S. Dubey, J. Singh and R. P. Singh, *Aspergillus niger* PA2: a novel strain for extracellular biotransformation of L-tyrosine into L-DOPA, *Amino Acids*, **48**, 1253 (2016).
20. S. Giannopoulou, K. Samardzica, B. B. A. Raymond, S. P. Djordjevic and K. J. Rodgersa, L-DOPA causes mitochondrial dysfunction in vitro: A novel mechanism of L- T DOPA toxicity uncovered, *Int. J. Biochem. Cell Biol.*, **117**, 105624 (2019).
21. A. G. Ibrahim, F. A. Hai, H. A. Wahab and H. Mahmoud, Synthesis, characterization, swelling studies and dye removal of chemically crosslinked acrylic acid/acrylamide/N,N-dimethyl acrylamide hydrogels, *Am. J. Appl. Chem.*, **4**, 221 (2016).
22. S. Li and G. Chen, Using hydrogel-biochar composites for enhanced cadmium removal from aqueous media, *Material Sci & Eng.*, **2**, 294 (2018).
23. K. K. Mali, S. C. Dhawale, R. J. Dias, N. S. Dhane and V. S. Ghorpade, Citric acid crosslinked carboxymethyl cellulose-based composite hydrogel films for drug delivery, *Indian J. Pharm. Sci.*, **80**, 657 (2018).
24. İ. Karaca Açarı, Investigation of the effectiveness of polyurethane composites containing gelatin at different rates on the release of ciprofloxacin, *J.Chem.Soc.Pak.*, **43**, 645 (2021).
25. Y. Z. Zhou, R. G. Alany, V. Chuang and J. Wen, Optimization of PLGA nanoparticles formulation containing L-DOPA by applying the central composite design, *Drug Dev Ind Pharm.*, **39**, 321 (2012).
26. M. Z. Ahmad, A. H. B. Sabri, Q. K. Anjani, J. Domínguez-Robles, N. A. Latip and K. A. Hamid, Design and development of levodopa loaded polymeric nanoparticles for intranasal delivery, *Pharmaceuticals*, **15**, 370 (2022).
27. J. Niu, F. Wang, X. Zhu, J. Zhao and J. Ma, One-pot synthesis of L-dopa-functionalized water-dispersible magnetite nano-palladium catalyst and its application in the Suzuki and Heck reactions in water: a novel and highly active catalyst, *RSC Adv.*, **4**, 37761 (2014).
28. A. M. Dumitrescu, G. Lisa, A. R. Iordan, F. Tudorache, I. Petrila, A. I. Borhan, M. N. Palamaru, C. Mihailescu, L. Leontie and C. Munteanu, Ni ferrite highly organized as humidity sensors, *Mater. Chem. Phys.*, **156**, 170 (2015).
29. S. Chauhan and L. S. B. Upadhyay, Biosynthesis of iron oxide nanoparticles using plant derivatives of *Lawsonia inermis* (Henna) and its surface modification for biomedical application, *Nanotechnol. Environ. Eng.*, **4**, 2 (2019).

30. P. Anandan, S. Vetrivel, S. Karthikeyan, R. Jayave and G. Ravi, Crystal growth, spectral and thermal analyses of a semi organic nonlinear optical single crystal: L-tyrosine hydrochloride, *Optoelectron. Adv. Mater. Rapid Commun.*, **6**, 1128 (2012).
31. J. Fan, Z. Shi, M. Lian, H. Li and J. Yin, Mechanically strong graphene oxide/sodium alginate/ polyacrylamide nanocomposite hydrogel with improved dye adsorption capacity, *J. Mater. Chem. A.*, **1**, 7433 (2013).
32. M. E. Cam, S. Yildiz, H. Alenezi, S. Cesur, G. S. Ozcan, G. Erdemir, U. Edirisinghe, D. Akakin, D. S. Kuruca, L. Kabasakal, O. Gunduz and M. Edirisinghe, Evaluation of burst release and sustained release of pioglitazone-loaded fibrous mats on diabetic wound healing: an in vitro and in vivo comparison study, *J. R. Soc. Interface*, **17**, 20190712 (2019).
33. F. Sabbagha and I. I. Muhamad, Acrylamide-based hydrogel drug delivery systems: Release of Acyclovir from MgO nanocomposite hydrogel, *J Taiwan Inst Chem Eng.*, **72**, 182 (2017).
34. L. Ferreira, M. M. Vidal and M. H. Gil, Design of a drug-delivery system based on polyacrylamide hydrogels. Evaluation of structural properties, *Chem. Educator.*, **6**, 100 (2001).
35. B. Singh, V. Sharma, R. Kumar and A. Kumar, Designing moringa gum-sterculia gum-polyacrylamide hydrogel wound dressings for drug delivery applications, *Carbohydrate Polymer Technologies and Applications.*, **2**, 100062 (2021).
36. A. C. Sintov, H. V. Levy and I. Greenberg, Continuous transdermal delivery of L-DOPA based on a self-assembling nanomicellar system, *Pharm Res.*, **34**, 1459 (2017).
37. M. M. Lakouraj, M. Rezaei and V. Hasantabar, Synthesis, characterization and in-vitro prolonged release of L-DOPA using a novel amphiphilic hydrogel based on sodium alginate-polypyrrole, *Int. J. Biol. Macromol.*, **193**, 609 (2021).
38. G. R. Bardajee, N. Khamooshi, S. Nasri and C. Vancaeyzeele, Multi-stimuli responsive nanogel/hydrogel nanocomposites based on κ -carrageenan for prolonged release of levodopa as model drug, *Int. J. Biol. Macromol.*, **153**, 180 (2020).
39. S. Thakur, G. S. Chauhan, J. H. Ahn, Synthesis of acryloyl guar gum and its hydrogel materials for use in the slow release of L-DOPA and L-tyrosine, *Carbohydr. Polym.*, **76**, 513 (2009).